ACS OMEGA

http://pubs.acs.org/journal/acsodf

Article

In Vitro and Silico Studies on the N-Doped Carbon Dots Potential in ACE2 Expression Modulation

Wiska Mailisa, Windy Dwi Annisa, Fitri Aulia Permatasari, Riezki Amalia, Atthar Luqman Ivansyah, Ferry Iskandar, and Heni Rachmawati*

Cite This: *ACS Omega* 2023, 8, 10077−10085

Read Online

ACCESS | Metrics & More | Article Recommendations | Supporting Information

ABSTRACT: The alteration of ACE2 expression level, which has been studied in many diseases, makes the topic of ACE2 inducer potential crucial to be explored. The ACE2 inducer could further be designed to control the ACE2 expression level, which is appropriate to a specific case. An in vitro study of well-characterized carbon dots (CDs), made from citric acid and urea, was performed to determine their ability to modulate the ACE2 receptor. Gene expression of ACE2 was quantified using concentrations adjusted for IC50 results from CDs viability assays in HEK 293 and A549 cell lines. RT-qPCR was used to assess the expression of the ACE2 gene and its induction effect in normal cell lines (HEK-293A). According to the results of the tests, ACE2 is expressed in HEK-293A cell lines, and diminazene aceturate can increase ACE2 expression. The effect of CDs on ACE2 gene expression was further examined on the cell lines that had previously been induced with diminazene aceturate, which resulted in upregulation of the ACE2 expression level. An in silico study has been done by using a molecular docking approach. The molecular docking results show that CDs can make strong interactions with ACE2 amino acid residues through hydrophobic interaction, $\pi-\pi$ interaction, π-cation interaction, and ionic interaction.

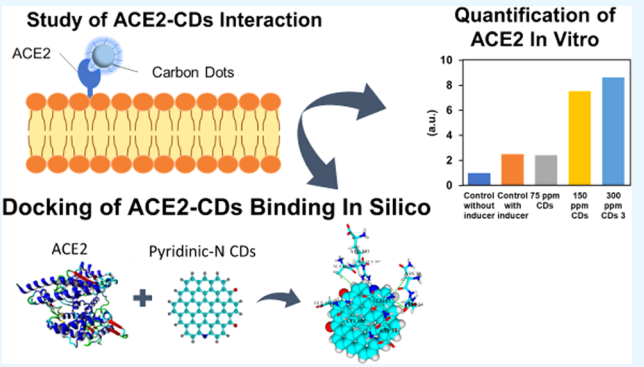

1. INTRODUCTION

Angiotensin converting enzyme 2 (ACE2) is a type-I transmembrane metallo-carboxypeptidase found in various human tissues and organs.[1−3] ACE2 is an integral membrane protein, an enzyme-linked receptor, which has an active site that faces the extracellular membrane and an enzyme site for catalytic function on the intracellular side.[4] Based on the registered database of ACE2 in GTEx Portal (https://www.gtexportal.org/), ACE2 gene expression is abundant in the adipose tissue, breast, small intestine, and testis, followed by the colon, heart, kidney, and lung in lower amounts, and many other tissues. ACE2, a homolog of angiotensin-converting enzyme (ACE), performs its function by converting Angiotensin-I (Ang-I) or Angiotensin-II (Ang-II), produced by ACE, into Ang (1−9) and Ang (1−7). The balance of the renin-angiotensin system between the deleterious axis (ACE/Ang-II/angiotensin type 1 receptor [AT1R]) and the vasoprotective axis (ACE2/Ang-(1−7)/Mas receptor [MasR]) is a pivotal condition to maintain cardiovascular homeostasis. Therefore, ACE2 may be relevant to a few diseases such as diabetes, lung injury, and fibrotic disease, as it has roles in counter-regulating the renin-angiotensin system (RAS).[5] Myocardial infarction (MI) causes imbalance in RAS due to the increase of the vasodilator axis and the decrease of the vasoprotective axis, which is indicated by the upregulation of ACE2 expression at the beginning as a compensatory mechanism and then a significant decrease in the heart failure stage.[6] A clinical study of ACE2 in individuals with diabetic kidney disease showed that the ACE2 protein expression level was lower than in healthy kidney patients (in both the tubulointerstitium and glomeruli).[7]

One of the common methods to determine the ACE2 expression level and activity is by quantifying the mRNA expression using RT-qPCR by the comparative $2^{-\Delta\Delta ct}$ method. This method calculates the relative fold gene expression of the samples and normalizes the mRNA expression to the endogenous reference gene β-actin.[8] Further analysis was conducted to study the ACE2 activity by quantifying the gene expression levels of AT1R, MasR, Ang 1−7, or Ang-II as a result of ACE2 activities in RAS.[8]

A few medicines called ACE inhibitors (ACEi) and angiotensin receptor blockers (ARBs) are used as therapeutic agents for cardiovascular diseases. Their therapeutic mecha-

Received: November 18, 2022
Accepted: February 22, 2023
Published: March 6, 2023

nism increases the ACE2 activity and further inhibits the deleterious axis of RAS. As one of the ARBs, the potential of diminazene aceturate (DIZE) has been studied to attenuate ischemia-induced cardiac pathophysiology since it could enhance ACE2 activity, which plays an essential role in myocardial infarction (MI). DIZE treatment showed a decrease in the infarct area and restored the normal balance of RAS.[6] In contrast, another mechanism of ACEi and ARB was found to inhibit kidney ACE with a reduction of ACE2 expression. Wysocki et al.[9] studied the effect of captropil and telmisartan treatment, and found a downregulation of ACE2 expression levels. Also, some other ACEi and ARB were reported to not affect ACE2 expression at protein levels of the kidney.[10]

Since ACE2 has a pivotal role as one of the RAS regulators, studying how any drug could modulate ACE2 would be an interesting topic. One of the interesting materials that have been studied regarding their interaction with ACE2 is carbon dots as a novel material in nanomedicine. It is well known that CDs have low toxicity, so they could potentially interact with ACE2 without affecting the cell mortality. Since they have varied functional groups and small particle sizes, CDs show enhanced potential to modulate ACE2.

A recent study of CDs related to cardiovascular disease studied the utility of their fluorescence and low toxicity for their use as a diagnostic agent for biothiol detection, indicating many disorders and diseases.[11] CDs also showed potential as a drug delivery or therapeutic agent in many studies. A study showed that combining curcumin with CDs can enhance the antiviral effect of EV21 in vitro and in vivo.[12] Several additional papers also mention the possibility of combining curcumin with CDs to prevent colon and breast cancer.[11,13] CDs have recently been a renewable fluorescent probe for molecular imaging. As a result, CDs can be considered a promising agent in the fight against viral infections. CDs have previously shown their capability to inhibit the HCoV-229E receptor.[14,15] Furthermore, the role of CDs in the therapy of infectious disorders such as the Human Immunodeficiency Virus (HIV), ebolavirus, and SARS-CoV is still being researched.[15] The potential of CDs in other biological uses is also being explored, including the study of cytotoxicity in breast cancer cell lines and as an anti-mycoplasma drug that can protect cells from infection due to their peroxidase catalytic activity.[16]

In this study, CDs were tried on the human embryonic kidney cell line HEK-293A to determine their potential in ACE2 expression modulation. The cytotoxicity assay was performed to calculate the IC50 of CDs on HEK-293A as a normal cell line and A549 as a cancer cell line to assess the potential of CDs as a therapeutic drug. This assay was also used as a preliminary investigation to ensure that the concentrations used to quantify ACE2 would not impair cell growth and development. ACE2 gene expression was also quantified without and with specific inducers to establish the presence of ACE2 expression and the influence of the inducer on the normal cell lines. This type of cell line is based on previous studies that have analyzed the distribution of ACE2 in renal cell lines (HEK-293A).[17] To confirm the modulation of ACE2 was induced by the CDs, we further analyzed the interaction between ACE2 and CDs in molecular scope by computational analysis. The potential of CDs as ACE2 modulators will be revealed as a result of this research, and they will be able to be used as a treatment approach for ACE2-related pathological illnesses.

2. MATERIALS AND METHODS

2.1. Materials. Materials: Citric acid (Sigma Aldrich), urea (Sigma Aldrich), DI water, HEK-293A and A549 cell lines (Collection of Cell and Molecular Biology Laboratory, Faculty of Pharmacy, Padjadjaran University), Dulbecco's Modified Eagle Medium (Sigma Aldrich), penicillin-streptomycin (PS) (Sigma Aldrich), fetal bovine serum (FBS) (Sigma Aldrich), phosphate buffer saline (Lonza), TrypLe (Gibco), Trypan blue solution (Sigma Aldrich), GoTaq-1-Step RT-qPCR System (Promega), Nuclease Free Water (Promega), ethanol (Merck), isopropanol (Sigma Aldrich), Ribozol RNA reaction reagent (Life Science), chloroform (Merck), ACE2 forward and reverse primers (Macrogen), GAPDH forward and reverse primers (Macrogen), Captopril (Kimia Farma), dexamethasone sodium phosphate (Phapros), Tryponil/1.05 g of diminazene aceturate, and 1.31 g of phenazone (Interchemie), Cell Counting Kit 8 (CCK-8), and aquades pro injection.

2.2. Synthesis of Carbon Dots. The synthesis process of CDs using the hydrothermal method is shown in Figure 1a.

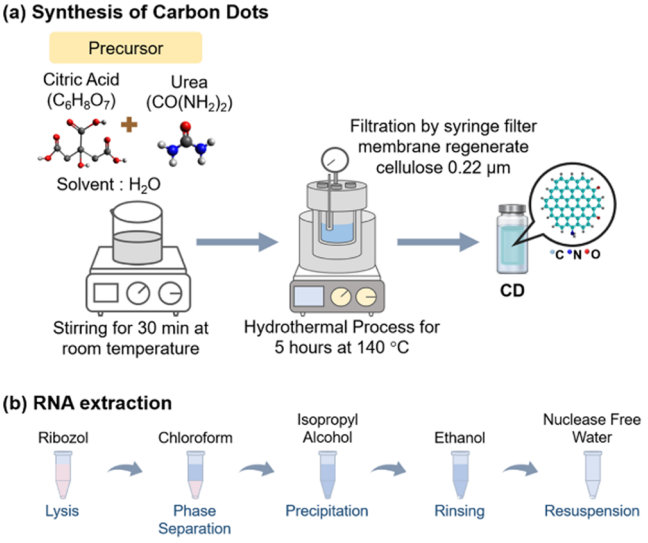

Figure 1. Method of experiment diagrams. (a) CDs synthesis process with the hydrothermal method; (b) RNA extraction process.

Citric acid and urea were dissolved in the deionized water by stirring for 30 min at room temperature. Then, the mixture was added to a hydrothermal tube and heated at 140 °C for 5 h. The colloid is filtered using a membrane syringe filter of 0.22 μm and then freeze-dried to collect the powder of CDs. CDs were stored at room temperature without exposure to direct light before further usage.

2.3. Carbon Dots' Characterization. The characterizations of CDs included size and morphology analysis, optical properties, functional group analysis, and surface charge measurement.

2.3.1. TEM Characterization. The size and morphology of the CDs were measured by a transmission electron microscope (TEM HT7700 Hitachi, Japan). The CDs were dispersed in water and dropped on the TEM grids (carbon-coated copper grids). After air drying the TEM grids, the images of the sample were taken at 120 keV. The particle size distribution of CDs was examined by measurement of ~100 particles' diameter using ImageJ software.

2.3.2. UV–Vis Absorption and PL Measurement. The absorbance of CDs was measured by the UV–vis spectropho-

https://doi.org/10.1021/acsomega.2c07398
ACS Omega 2023, 8, 10077−10085

tometer (UV−Vis N4S, China) with a range of 200−800 nm. Then, a fluorescence spectrophotometer (G9880A Fluorescence Spectrophotometer Agilent) was used to measure the emission and excitation spectra of CDs with an excitation slit width of 5 nm and an emission slit width of 5 nm. The fluorescence behavior of excitation dependency was measured by choosing an excitation range of 340−500 nm with a 25 nm increment.

2.3.4. FTIR Characterization. The functional groups contained in the CDs' structure were analyzed by mixing the sample with KBr into a pellet and further measured by a Fourier transform infrared spectrometer (FTIR, Bruker α, Germany) around the range of 4000−400 cm^{-1}.

2.3.5. Zeta Potential Measurement. Zeta Potential measurements were used to determine the surface charge of CDs. Around 1 ml of the sample was filled into the zeta cell. The measurements were performed using a zeta potential analyzer, Horiba SZ-100, for three replication times.

2.4. Cell Interaction Study of the Carbon Dot. *2.4.1. Cell Culture.* Human lung adenocarcinoma cells (A549) and human embryonic kidney 293 cells (HEK-293A) were grown in Dulbecco's modified Eagle's medium (DMEM) supplemented with 15% FBS and 1% PS solution in a humidified 37 °C, 5% CO_2 incubator.

2.4.2. Cell Viability Assay. The HEK-293A and A549 cell lines were grown at 15,000 cells per well in the 96-well plate. The cells were cultured for 24 h with different dosages of CDs in water. The media was then replaced with a CCK-8 reagent, and the cells were incubated for 2 h. At a wavelength of 450 nm, absorption analysis was performed using a Spectrophotometer-Tecan Nanoquant Microplate Reader, and cytotoxicity calculations were performed using the equation IC50 = $(50 - b)/a$, where a and b were determined from the equations of the cytotoxicity test graph line.

2.4.3. Identification of ACE2 Expression after Induction. The human embryonic kidney cell line HEK-293A was cultured in DMEM media containing 10% FBS and 1% penicillin-streptomycin in an incubator at 37 °C and 5% CO_2. Furthermore, 35×10^4 cells/well were seeded into 6-well plates and incubated for 24 h. The media was then replaced with a mix of media and each of the inducers, including captopril (Abuohashish et al., 2017), dexamethasone sodium phosphate (Sinha et al., 2020), diminazene aceturate (Tao et al., 2016), and PBS as a control. Then, the RNA from the cell line was extracted after 24 h according to the RNA extraction procedure. The GoTaq-1-step RT-qPCR system (Promega) technique was used to carry out the quantification process. Table S1 shows the primers used in this study.

2.4.4. Study of ACE2 modulation by Carbon Dots. The HEK-293A cell lines were maintained in a DMEM medium containing 10% FBS and 1% penicillin-streptomycin in an incubator at 37 °C and 5% CO_2. Furthermore, seeding was carried out in 6-well plates with concentrations of 35×10^4 cells/well, and then cultured for 24 h. Then, the initial medium was replaced with a mixture of media with diminazene aceturate as an ACE2 inducer. After the induction process for 24 h, the media was replaced with a mixture of media with CDs (75, 150, and 300 ppm) and then incubated again for 24 h. RNA from the cells with the test sample was extracted according to the RNA extraction procedure. The Ribozol RNA reaction reagent (Life Science) protocol was used for RNA extraction, which had been tweaked through an optimization process.[18] The extraction procedure is shown in Figure 1b. The GoTaq-1-step RT-qPCR system (Promega) technique was used to perform the quantification process. The primer used is shown in Table S1.

2.5. In Silico Study of Carbon Dots and ACE2 Interaction. *2.5.1. Preparation and Optimization of the Ligand and Receptor Structure.* The ligands used in this study consisted of CDs, where the CDs were modeled by using the N-pyridinic, N-pyrrolic, and N-graphitic forms of the CDs, as shown in Figure 2b−d, respectively. The three-dimensional

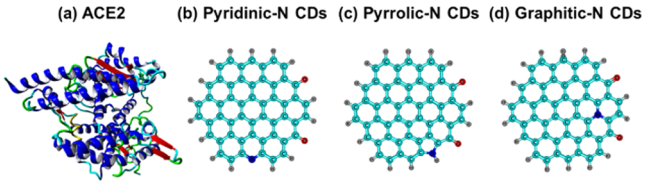

Figure 2. Structure of (a) angiotensin-converting enzyme 2 (ACE2), (b) graphitic-N form of carbon dots, (c) pyridinic-N form of carbon dots, (d) pyrrolic-N form of carbon dots.

structure of ACE2 was obtained from a database of The Research Collaboratory for Structural Bioinformatics Protein Data Bank (RSCB PDB) (https://www.rscb.org) in PDB file format. The code structure used is 6M0J, chain A, as shown in Figure 2a. The ligand molecule was created with the help of Avogadro software version 1.2.0.[19] Furthermore, the ligand molecule was optimized using the DFT method with B3LYP-D4 functional and the def2-TZVP basis set using ORCA version 5.0.3 software package.[20] The ACE2 receptor was minimized using the em_run.mcr macro on YASARA software version 22.5.22 with AMBER14 force field.[21,22]

2.5.2. Molecular Docking. The next step in this research is to dock the ligand molecule to the ACE2 receptor molecule. Molecular docking studies were carried out using YASARA software version 22.5.22 with the VINA molecular docking method.[23] Before molecular docking, system optimization was carried out by removing water molecules, adding and distributing the partial charge of the atoms using the Kollman method, and adding polar hydrogen atoms. The other parameters were set according to the default values. The conformers from molecular docking were further analyzed to determine the hydrogen bonding, Van der Waals forces, hydrophobic interactions, and electrostatic interactions. YASARA implements a scoring function, where the more positive the binding affinity value of a ligand on the receptor, the better, because the more strongly does the ligand bind noncovalently to the binding pocket receptor.[21,24] The active site of the ACE2 receptor, which becomes the binding pocket for the ligand, consists of amino acid residues that interact with the spike protein of SARS-CoV-2, namely Serine 19, Glutamine 24, Threonine 27, Proline 28, Aspartic Acid 30, Lysine 31, Phenylalanine 32, Histidine 34, Glutamic Acid 35, Aspartic Acid 38, Phenylalanine 40, Tyrosine 41, Glutamine 42, Leucine 45, Methionine 82, Tyrosine 83, Asparagine 330, Leucine 351, Glycine 352, Lysine 353, Glycine 354, Aspartic Acid 355, Arginine 357, Alanine 386, and Arginine 393.[25]

3. RESULTS AND DISCUSSION

3.1. Synthesis and Characterization of CDs. Carbon dots (CDs), an emerging nanomaterial with excellent biocompatibility, were synthesized by the hydrothermal process. Figure 3 shows that the as-synthesized sample is in

https://doi.org/10.1021/acsomega.2c07398
ACS Omega 2023, 8, 10077−10085

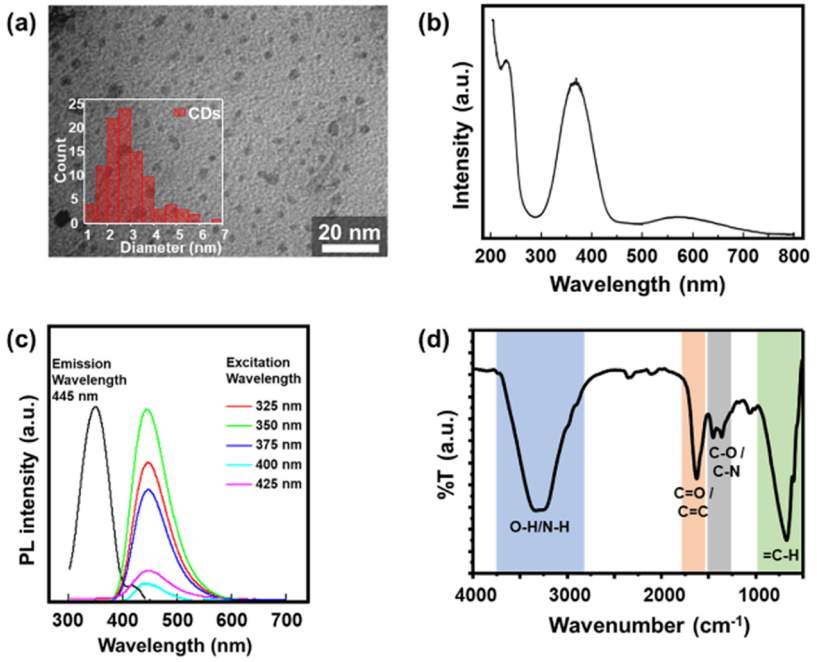

Figure 3. CDs characterization. (a) TEM image and size distribution graph of CDs. (b) Absorbance spectrum of CDs. (c) Excitation and emission spectra of CDs. (d) FTIR spectrum of CDs.

dark green with blue emission under UV excitation. The color of the CDs solution produced in this synthesis is dark green, in accordance with the general photoluminescence color of CDs, which is green or blue.[26,27] The TEM characterization results showed the typical CDs with the size of ∼2.9 nm (Figure 3a).[28,29] The particle size distribution of CDs ranged between 1 and 7 nm. The morphology of the CDs displayed typical spherical particles in the TEM images. ACE2 comprises a 805 amino acid (AA) type-I transmembrane protein, which is 110−120 kDa in molecular weight and ∼3 nm in length.[30] This size is similar to our synthesized material, CDs, increasing the potential of this nanoparticle to interact with the receptor without any steric obstacle.

The absorbance spectra of the CDs showed peaks at wavelengths of 220 and 360 nm (Figure 3b). These findings are consistent with earlier research on the properties of the CDs.[31] In addition to these wavelengths, there is a modest peak at 650 nm, which is part of the NIR window area and is used in cancer therapy. Emission measurements were also carried out at an excitation wavelength of 365 nm and produced a peak at 460 nm (Figure 3c). At this wavelength, the CDs produce a blue glow. The results of this characterization also resemble the previous CDs study in which the blue glow produced under 365 nm UV exposure indicated that CDs have been formed.[32] The CDs also showed excitation-independent behavior with the highest fluorescence intensity at 350 nm of excitation wavelength. The synthesized CDs have an abundance of the O−H/N−H functional group, as shown in Figure 3d, with a broad peak at 3000−3500 cm^{-1}. The peak at 1628 cm^{-1} indicated that the C═O/C═C functional group involved in the conjugated double bond of carbon with the C-O/C-N at 1454 and 1363 cm^{-1} resulted in the fluorescence of CDs after lightening by the UV beam.[33,34] As reported in our previous work, these typical CDs plausibly consist of various C−N configurations, including Pyridinic-N, Pyrrolic-N, Graphitic-N, and Amino-N, on their surfaces.[35] Therefore, it is highly plausible that the as-prepared CDs are N-doped CDs rather than pristine CDs.

3.2. Viability Assay of Carbon Dots on Normal and Cancer Cells. CDs viability assay was performed on HEK-293A and A549 cell lines with various concentrations. The viability assay chart is shown in Figures 4. The correlation

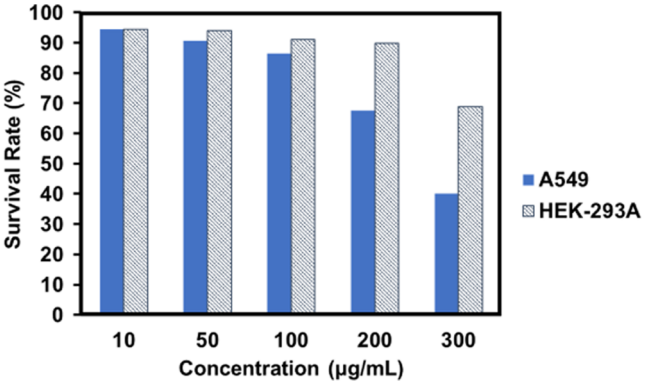

Figure 4. Graph of CDs' viability assay on HEK-293A and A549.

between concentration and cell viability could be well suited for second-order polynomial models with a regression of >0.9. The equation IC50 = $(50 - b)/a$ was used to calculate the IC50 of CDs. The decision to use this cell line was based on a prior study that found ACE2 in kidney cells[36] and respiratory cells.[37] The assay results were conducted to establish safe concentration limits for cells to assess the effects of CDs on ACE2 levels.[38]

The state of the cells before and after treatment with various concentrations of CDs is shown in Figure S1. As the doses of CDs increased, the density of HEK-293A cells decreased, as shown in Figure S1. The CDs showed compatibility in the normal cell with a half maximum inhibitory concentration (IC_{50}) of 0.378 and 0.263 mg/mL in HEK-293A and A549 cell

https://doi.org/10.1021/acsomega.2c07398
ACS Omega 2023, 8, 10077−10085

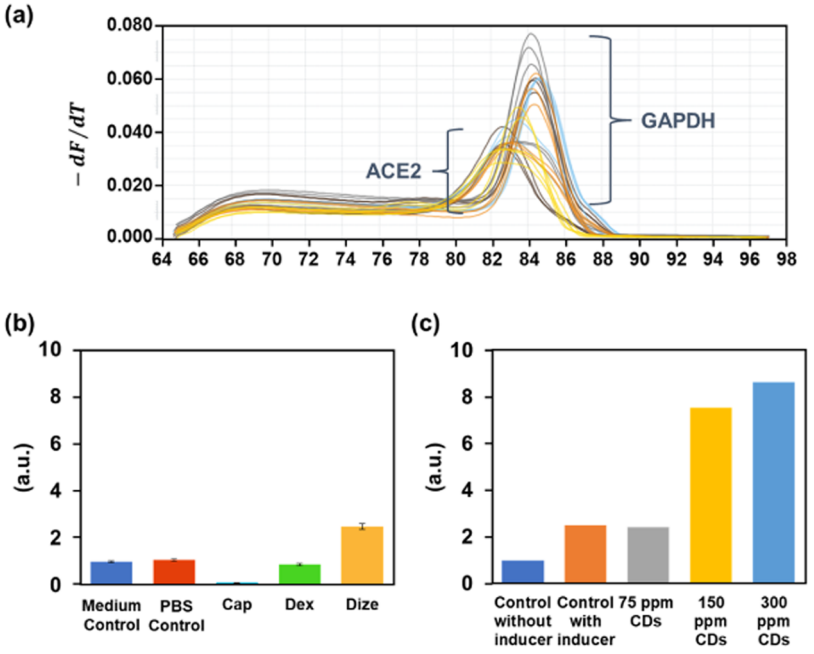

Figure 5. Result of ACE2 modulation in HEK-293A cell lines. (a) Melting curve of ACE2 in HEK-293A using RT-qPCR. (b) Quantification of ACE2 modulation by inducers in HEK-293A cell lines. (c) Quantification of ACE2 modulation by CDs in HEK-293A cell lines after induction.

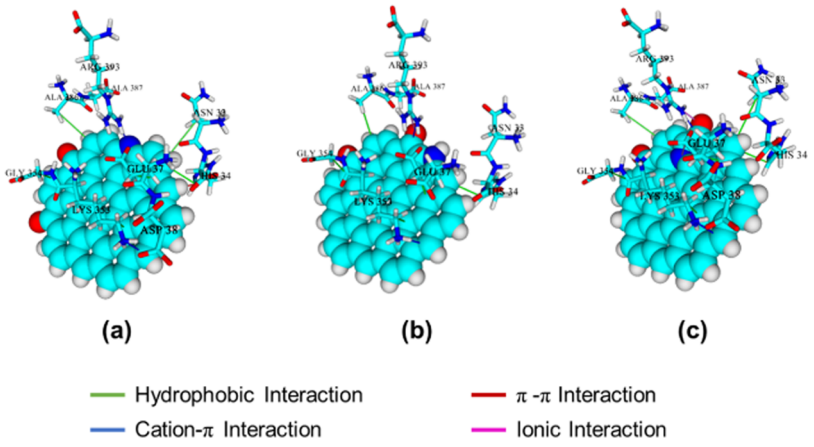

Figure 6. Interaction of ACE2 amino acid residue with the (a) Graphitic-N form of carbon dots, (b) Pyridinic-N form of carbon dots, and (c) Pyrrolic-N form of carbon dots from the molecular docking results.

lines, respectively. CDs are more potent in cancer cells than in normal cells at relatively high doses. Some reports showed that CDs have low toxicity to normal cells. Thus, it could be a promising drug delivery agent.[39]

3.3. Modulation of ACE2 in the HEK-293A cell line with Carbon Dot. The results for the purity of the HEK-293A RNA extraction for quantification of ACE2 are shown in Tables S2 and S3 for inducer treatment and CDs treatment, respectively. The acceptable ratio of A260/280 pure RNA is ∼2.0.

The lower ratio achieved in these two assays (Tables S2 and S3) indicated that the sample was contaminated by the leftover chemicals used in the extraction process. The melting curve in the HEK 293A cell lines gave rise to peaks at the same temperature, according to the test results; a complete depiction is shown in Figure 5a and S2. The presence of peaks at the same temperature suggests that the analysis method revealed a single product that is either particular or free of contamination. The effects of CDs at various concentrations on the ACE2 of the HEK-293A cell line are then compared, revealing a difference in the ratio (Figure 5c).

The potent concentration of CDs to modulate the ACE2 expression level, after being induced by DIZE (the highest upregulator of ACE2 in Figure 5b), was started from 150 ppm since there was no significant increase in ACE2 expression. As the concentration of CDs increased, the ACE2 expression level also increased much higher than that of its inducer. Therefore, CDs, which has similar potential as DIZE, could be utilized in some cardiovascular cases that need to balance the RAS. The previous report showed that upregulation of ACE2 activity by induction in vivo could lower the vasoconstriction of the Ang-II effect, leading to reduced blood pressure. Wang et al. (2021) studied the potential of DIZE to protect ACE2 enzyme activity during lung ischemia-reperfusion (IR) injury in vitro and in vivo.[40] Based on a review of ACEi and ARB medicines found to protect against acute lung injury (ALI), some reports showed that the ACE2 in tissues could be upregulated by ACEi, while the ARB upregulated the urinary ACE2 level.[41]

https://doi.org/10.1021/acsomega.2c07398
ACS Omega 2023, 8, 10077−10085

The upregulation of ACE2 by perindopril, one of the ACEi, was studied for liver fibrosis therapy and resulted in hepatic function improvement due to the increase of the ACE2-Ang (1−7)-MAS axis.[42] However, this result could be different from the complete system in vivo; hence, further analysis should be conducted to get an appropriate interpretation.

3.4. Molecular Interaction Study of Carbon Dots and ACE2. Carbon dot (CDs)-derived ligands in this investigation were screened for their inhibitory ability against ACE2, with the optimized structure shown in Figure 6. Pyridinic-N, Pyrrolic-N, and Graphitic-N CDs are a variation of N-doped CDs, which are attractive to be explored in previous studies and applications.[35,43,44] The results of docking using YASARA software on the four ligand compounds and ACE2 yielded data with binding energy values. The binding energy is calculated using an empirical equation as shown in eq 1.[45]

$$\Delta G = \Delta G_{vdW} + \Delta G_{Hbond} + \Delta G_{elec} + \Delta G_{tor} + \Delta G_{desolv} \quad (1)$$

where ΔG_{vdW} is the van der Waals term in the docking energy, ΔG_{Hbond} is the hydrogen bond term, ΔG_{elec} is the electrostatic term, ΔG_{tor} is the torsional free energy term of a compound when the compound moves from the unbound state to the bonded state, and ΔG_{desolv} is the de-solvation term for the docking energy.

The more positive value of binding energy indicates that the affinity of the ligand to the ACE2 receptor is better according to the YASARA scoring convention (Krieger and Vriend, 2014, 2015). In other words, the more positive the binding energy value, the more stable the interaction between these ligands and ACE2. In addition, the more positive the binding energy value, the stronger the bond between the ligand and the receptor. The data obtained from the docking result, the summary of the interaction type, the total interaction number and strength of hydrophobic interaction, $\pi-\pi$ interaction, π-cation interaction, and ionic interaction between five ligand compounds with ACE2 can be seen in Tables S4−S9, respectively.

These data show that all of the ligands have positive values. This indicates that they could make strong interactions with the ACE2 receptor. Table S4 shows that the interaction between CD ligands and the ACE2 receptor has a binding energy value of 10.677, 10.529, and 10.567 for Pyridinic-N CDs, Pyrrolic-N CDs, and Graphitic-N CDs, respectively. These values indicate that the Pyridinic-N CDs ligands have stronger and more stable interactions with ACE2. The potential of ligand compounds as ACE2 inducers can be studied further by analyzing other data generated from the molecular docking process, such as binding position, type of bond, distance, and ACE2 amino acid residues involved in bonding with the ligand compounds.

YASARA Structure software was also used for further identification to analyze the most relevant interactions from the closest interatomic distance. The results of this analysis can be seen in Figure 6 and Tables S4−S9. Based on these data, it is known that the Pyridinic-N CD ligand compound, which has the best affinity when compared to other ligands, was also able to form hydrophobic interactions with ASN 33, HIS 34, GLU 37, LYS 353, GLY 354, and ALA 386, which have the average strength of 3.379. Similar to other CD ligands, this ligand is also capable of forming π-π interaction with HIS 34 and π−cation interaction with LYS 353 and ARG 393, which have an average strength of 6.668 and 3.201, respectively. However, there is no ionic interaction between Pyridinic-N CDs and ACE2 amino acid residues. The Pyrrolic-N CDs are capable of forming hydrophobic bonds with residues of HIS 34, GLU 37, LYS 353, GLY 354, and ALA 386; $\pi-\pi$ interaction with HIS 34; π−cation interaction with LYS 353 and ARG 393; and ionic interaction with ARG 393, with average interaction strengths of 4.399, 5.155, 2.003, and 0.584, respectively. There are more than 10 total interaction numbers for the strongest interaction between the CD ligand and ACE2 receptor amino acid residues, which make the CD ligand have a strong interaction with the ACE2 receptor. The last CD ligand compound, Graphitic-N CD ligand, formed hydrophobic interactions with ASN 33, HIS 34, GLU 37, LYS 353, GLY 354, and ALA 386 residues; π-π interaction with HIS 34; and π-cation interaction with LYS 353 and ARG 393. However, besides ARG 393, GLU 37 also contributed to forming ionic interaction with Graphitic-N CDs. These interactions have an average strength of 3.778, 6.671, 2.695, and 0.431 for hydrophobic, $\pi-\pi$, π-cation, and ionic interaction, respectively.

These molecular docking results indicate that most of the interactions between the Pyridinic-N CDs, Pyrrolic-N CDs, and Graphitic-N CDs ligands and ACE2 occur at residues HIS 34, GLU 37, PHE 40, SER 43, SER 44, TRP 69, TRP 349, LYS 353, GLY 354, PHE 390, LEU 391, and ARG 393. These residues are located around the active site of the ACE2 enzyme since the active site consists of Serine 19, Glutamine 24, Threonine 27, Proline 28, Aspartic Acid 30, Lysine 31, Phenylalanine 32, Tyrosine 41, Glutamine 42, Leucine 45, Methionine 82, Tyrosine 83, Asparagine 330, Leucine 351, Glycine 352, Lysine 353, Glycine 354, Aspartic Acid 355, Arginine 357, Alanine 386, and Arginine 393.[25] This result indicates that carbon dot ligands can be promising inhibitors to inhibit the activity of the ACE2 enzyme.

3.5. Discussion. Carbon dots (CDs) have been attractive to be explored since their modification showed advantages in biomedicine applications. Many researchers tried to improve the lack of efficacy from small-molecule drugs (molecular weight in the range of 0.1−1 kDa) by creating nanoparticles with graphene-like structures as a core that have functional groups as the active site. This kind of structure was proposed to be composed of carbon dots that are 1−10 nm in size and typically have fluorescence. The alteration of small molecules to nanoparticle size, surface charge, and structure may give considerable pharmacological effects. It may reduce the toxicity, have a specific binding site, and extend the circulation time in the blood.[46] Many studies have been conducted to look for the appropriate application of specific disease treatment using CDs.

ACE2 regulation by specific inducers is considered to be explored since it is one of the pivotal components of RAS. ACE2 is a biomacromolecule that catalyzes Ang-II degradation to yield Ang (1−7), which balances the vasoconstrictor effect of the ACE-Ang-II axis.[47] The details of ACE2's roles in RAS are shown in Figure 7. Some inducers are known to alter the catalytic activities of ACE2 by changing its structure. The structure alteration could be due to the conformation change or a change in the bonding pattern of ACE2. Kulemina and Ostrov predicted the conformational shuffling of ACE2 because of modulation by three Food and Drug Administration (FDA)-approved compounds: hydroxyzine (HXZ), minithixen (CTX), and diminazene (DMZ).[48] The results showed that those compounds could bind to the ACE2 receptor, which is the active site, and change the substrate specificity. This

https://doi.org/10.1021/acsomega.2c07398
ACS Omega 2023, 8, 10077−10085

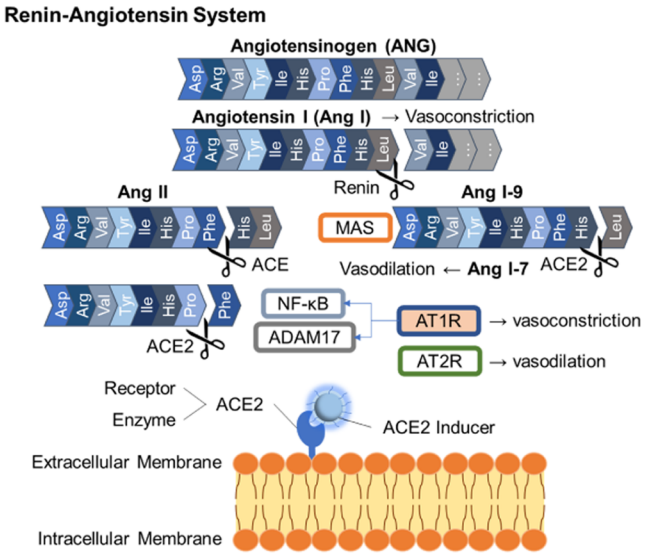

Figure 7. Role of ACE2 in RAS and the illustration of ACE2 and CDs interaction.

alteration was in conformity with the rate-limiting hypothesis of substrate binding or product release.

The synthesized CDs showed potential to modulate the ACE2 expression level due to their interactions as per the dose-dependent experimental results. ACE2 expression level could be upregulated by 150 ppm of the CDs concentration after being induced by DIZE. The molecular analysis of this event was consistent with the computational results that CD-containing nitrogen strongly interacts with the ACE2 receptor. The experimental results showed that the functional group containing nitrogen from the urea precursor could be one of the reasons for ACE2 modulation. Any kind of nitrogen position in the structure of CDs is considered to affect the interaction between ACE2 and CDs, as shown in the computational result, which could further improve the CDs synthesis.[35] The low toxicity of these CDs to the normal cell line and their capability to enhance ACE2 activity suggest that they could be a promising treatment for high blood pressure or hypertension with fewer side effects.

4. CONCLUSIONS

As a kind of new nanoparticles with low toxicity, the CDs show potential to modulate ACE2 by upregulating the gene expression level by up to 150 ppm of the CDs concentration after being induced by DIZE. This preliminary research data on the effect of modulating CDs on ACE2 in the HEK-293A cell lines might be considered a reference for further research. From an in silico study using the molecular docking approach, it has been shown that CDs can make strong interactions with ACE2 receptor amino acid residues, with the binding energy values of 10.677, 10.529, and 10.567 kcal/mol for the interactions of ACE2 receptor amino acid residues with Pyridinic-N CDs, Pyrrolic-N CDs, and Graphitic-N CDs, respectively. These results suggest that the interaction between CDs and ACE2 resulted in the upregulation of ACE2 gene expression level, potentially giving a protective therapeutic effect for cardiovascular-related diseases. Further studies need to be carried out to prove how CDs are involved in RAS, which is correlated to the balance of ACE/Ang-II/angiotensin type 1 receptor [AT1R] and ACE2/Ang-(1−7)/Mas receptor [MasR] complexes.

■ ASSOCIATED CONTENT

Supporting Information

The Supporting Information is available free of charge at https://pubs.acs.org/doi/10.1021/acsomega.2c07398.

Detailed primer of ACE2 and GAPDH used in this study, ACE2 quantification, and docking result of the ACE2 interaction with CDs ligands (PDF)

■ AUTHOR INFORMATION

Corresponding Author

Heni Rachmawati − *Research Group of Pharmaceutics - School of Pharmacy, Institut Teknologi Bandung, Bandung 40132, Indonesia; Research Center for Nanosciences and Nanotechnology, Institut Teknologi Bandung, Bandung 40132, Indonesia;* orcid.org/0000-0003-1968-0002; Email: hrachma@yahoo.com

Authors

Wiska Mailisa − *Research Group of Pharmaceutics - School of Pharmacy, Institut Teknologi Bandung, Bandung 40132, Indonesia*

Windy Dwi Annisa − *Research Center for Nanosciences and Nanotechnology, Institut Teknologi Bandung, Bandung 40132, Indonesia;* orcid.org/0000-0002-2092-5989

Fitri Aulia Permatasari − *Department of Physics, Faculty of Mathematics and Natural Sciences, Institut Teknologi Bandung, Bandung 40132, Indonesia; Research Center for Chemistry, National Research and Innovation Agency, BRIN, Kawasan Puspiptek 15314 Banten, Indonesia;* orcid.org/0000-0002-3228-8307

Riezki Amalia − *Department of Pharmacology and Clinical Pharmacy, Padjadjaran University, Jatinangor 45363, Indonesia*

Atthar Luqman Ivansyah − *Analytical Chemistry Research Group, Department of Chemistry, Faculty of Mathematics and Natural Sciences, Institut Teknologi Bandung, Bandung 40132 West Java, Indonesia*

Ferry Iskandar − *Research Center for Nanosciences and Nanotechnology, Institut Teknologi Bandung, Bandung 40132, Indonesia; Department of Physics, Faculty of Mathematics and Natural Sciences, Institut Teknologi Bandung, Bandung 40132, Indonesia; Collaboration Research Center for Advanced Energy Materials, National Research and Innovation Agency - Institut Teknologi Bandung, Bandung 40132 West Java, Indonesia;* orcid.org/0000-0002-0464-0035

Complete contact information is available at: https://pubs.acs.org/10.1021/acsomega.2c07398

Author Contributions

W.M.: investigation, data curation, formal analysis, writing − original draft. W.D.A.: characterization, formal analysis, visualization, writing − review & editing. F.A.P.: resources, writing − review & editing. R.A.: supervision, resource, formal analysis, writing − review & editing. A.L.I.: formal analysis, writing − review & editing. F.I.: supervision, funding acquisition, writing − review & editing. H.R.: conceptualization, formal analysis, supervision, writing − review & editing.

https://doi.org/10.1021/acsomega.2c07398
ACS Omega 2023, 8, 10077−10085

Notes

The authors declare no competing financial interest.

■ ACKNOWLEDGMENTS

This work was fully supported by the Indonesian Endowment Fund for Education and the Indonesian Science Fund through the International Collaboration RISPRO Funding Program Grant No. RISPRO/KI/B1/KOM/11/4542/2/2020.

■ REFERENCES

(1) Harmer, D.; Gilbert, M.; Borman, R.; Clark, K. L. Quantitative MRNA Expression Profiling of ACE 2, a Novel Homologue of Angiotensin Converting Enzyme. *FEBS Lett.* **2002**, *532*, 107−110.
(2) Eur J Clin Investigation − 2009 - Oudit - SARS-coronavirus Modulation of Myocardial ACE2 Expression and Inflammation in.Pdf.
(3) Riordan, J. F. Angiotensin-I-Converting Enzyme and Its Relatives. *Genome Biol* **2003**, *4*, No. 225.
(4) Warner, F. J.; Smith, A. I.; Hooper, N. M.; Turner, A. J. Angiotensin-Converting Enzyme-2: A Molecular and Cellular Perspective. *Cell. Mol. Life Sci.* **2004**, *61*, 2704−2713.
(5) Samavati, L.; Uhal, B. D. ACE2, Much More Than Just a Receptor for SARS-COV-2. *Front. Cell Infect. Microbiol.* **2020**, *10*, No. 317.
(6) Qi, Y.; Zhang, J.; Cole-Jeffrey, C. T.; Shenoy, V.; Espejo, A.; Hanna, M.; Song, C.; Pepine, C. J.; Katovich, M. J.; Raizada, M. K. Diminazene Aceturate Enhances Angiotensin-Converting Enzyme 2 Activity and Attenuates Ischemia-Induced Cardiac Pathophysiology. *Hypertension* **2013**, *62*, 746−752.
(7) Mizuiri, S.; Hemmi, H.; Arita, M.; Ohashi, Y.; Tanaka, Y.; Miyagi, M.; Sakai, K.; Ishikawa, Y.; Shibuya, K.; Hase, H.; Aikawa, A. Expression of ACE and ACE2 in Individuals with Diabetic Kidney Disease and Healthy Controls. *Am. J. Kidney Dis.* **2008**, *51*, 613−623.
(8) Tao, L.; Qiu, Y.; Fu, X.; Lin, R.; Lei, C.; Wang, J.; Lei, B. Angiotensin-Converting Enzyme 2 Activator Diminazene Aceturate Prevents Lipopolysaccharide-Induced Inflammation by Inhibiting MAPK and NF-KB Pathways in Human Retinal Pigment Epithelium. *J. Neuroinflammation* **2016**, *13*, No. 35.
(9) Wysocki, J.; Lores, E.; Ye, M.; Soler, M. J.; Batlle, D. Kidney and Lung ACE2 Expression after an ACE Inhibitor or an Ang II Receptor Blocker: Implications for COVID-19. *J. Am. Soc. Nephrol.* **2020**, *31*, 1941−1943.
(10) Cahova, M.; Kveton, M.; Petr, V.; Funda, D.; Dankova, H.; Viklicky, O.; Hruba, P. Local Angiotensin-Converting Enzyme 2 Gene Expression in Kidney Allografts Is Not Affected by Renin-Angiotensin-Aldosterone Inhibitors. *Kidney Blood Pressure Res.* **2021**, *46*, 245−249.
(11) Khan, F. A.; Lammari, N.; Muhammad Siar, A. S.; Alkhater, K. M.; Asiri, S.; Akhtar, S.; Almansour, I.; Alamoudi, W.; Haroun, W.; Louaer, W.; et al. Quantum Dots Encapsulated with Curcumin Inhibit the Growth of Colon Cancer, Breast Cancer and Bacterial Cells. *Nanomedicine* **2020**, *15*, 969−980.
(12) Lin, C. J.; Chang, L.; Chu, H. W.; Lin, H. J.; Chang, P. C.; Wang, R. Y. L.; Unnikrishnan, B.; Mao, J. Y.; Chen, S. Y.; Huang, C. C. High Amplification of the Antiviral Activity of Curcumin through Transformation into Carbon Quantum Dots. *Small* **2019**, *15*, No. 1902641.
(13) Sawant, V. J.; Bamane, S. R.; Kanase, D. G.; Patil, S. B.; Ghosh, J. Encapsulation of Curcumin over Carbon Dot Coated TiO2 Nanoparticles for PH Sensitive Enhancement of Anticancer and Anti-Psoriatic Potential. *RSC Adv* **2016**, *6*, 66745−66755.
(14) Łoczechin, A.; Séron, K.; Barras, A.; Giovanelli, E.; Belouzard, S.; Chen, Y. T.; Metzler-Nolte, N.; Boukherroub, R.; Dubuisson, J.; Szunerits, S. Functional Carbon Quantum Dots as Medical Countermeasures to Human Coronavirus. *ACS Appl. Mater. Interfaces* **2019**, *11*, 42964−42974.
(15) Manivannan, S.; Ponnuchamy, K. Quantum Dots as a Promising Agent to Combat COVID-19. *Appl. Organomet. Chem.* **2020**, *34*, No. e5887.
(16) Jiang, F.; Chen, D.; Li, R.; Wang, Y.; Zhang, G.; Li, S.; Zheng, J.; Huang, N.; Gu, Y.; Wang, C.; Shu, C. Eco-Friendly Synthesis of Size-Controllable Amine-Functionalized Graphene Quantum Dots with Antimycoplasma Properties. *Nanoscale* **2013**, *5*, 1137−1142.
(17) Bártová, E.; Legartová, S.; Krejčí, J.; Arcidiacono, O. A. Cell Differentiation and Aging Accompanied by Depletion of the ACE2 Protein. *Aging* **2020**, *12*, 22495−22508.
(18) Sultan, M.; Amstislavskiy, V.; Risch, T.; Schuette, M.; Dökel, S.; Ralser, M.; Balzereit, D.; Lehrach, H.; Yaspo, M.-L. Influence of RNA Extraction Methods and Library Selection Schemes on RNA-Seq Data. *BMC Genomics* **2014**, *15*, No. 675.
(19) Hanwell, M. D.; Curtis, D. E.; Lonie, D. C.; Vandermeerschd, T.; Zurek, E.; Hutchison, G. R. Avogadro: An Advanced Semantic Chemical Editor, Visualization, and Analysis Platform. *J. Cheminf.* **2012**, *4*, No. 17.
(20) Neese, F.; Wennmohs, F.; Becker, U.; Riplinger, C. The ORCA Quantum Chemistry Program Package. *J. Chem. Phys.* **2020**, *152*, No. 224108.
(21) Krieger, E.; Vriend, G. YASARA View—Molecular Graphics for All Devices—from Smartphones to Workstations. *Bioinformatics* **2014**, *30*, 2981−2982.
(22) Maier, J. A.; Martinez, C.; Kasavajhala, K.; Wickstrom, L.; Hauser, K. E.; Simmerling, C. Ff14SB: Improving the Accuracy of Protein Side Chain and Backbone Parameters from Ff99SB. *J. Chem. Theory Comput.* **2015**, *11*, 3696−3713.
(23) Trott, O.; Olson, A. J. AutoDock Vina: Improving the Speed and Accuracy of Docking with a New Scoring Function, Efficient Optimization, and Multithreading. *J. Comput. Chem.* **2010**, *31*, 455−461.
(24) Krieger, E.; Vriend, G. New Ways to Boost Molecular Dynamics Simulations. *J. Comput. Chem.* **2015**, *36*, 996−1007.
(25) Franz, A. W. E.; Sparagano, O.; Ortega, J. T.; Jastrzebska, B.; Rangel, H. R. Omicron SARS-CoV-2 Variant Spike Protein Shows an Increased Affinity to the Human ACE2 Receptor: An In Silico Analysis. *Pathogens* **2021**, *11*, No. 45.
(26) Shahdeo, D.; Roberts, A.; Abbineni, N.; Gandhi, S. *Graphene Based Sensors*, 1st ed.; Elsevier B.V., 2020; Vol. *91* DOI: 10.1016/bs.coac.2020.08.007.
(27) Muyassiroh, D. A. M.; Permatasari, F. A.; Iskandar, F. Machine Learning-Driven Advanced Development of the Carbon-Based Luminescent Nanomaterials. *J. Mater. Chem. C* **2022**, *10*, 17431−17450.
(28) Permatasari, F. A.; Aimon, A. H.; Iskandar, F.; Ogi, T.; Okuyama, K. Role of C-N Configurations in the Photoluminescence of Graphene Quantum Dots Synthesized by a Hydrothermal Route. *Sci. Rep.* **2016**, *6*, No. 21042.
(29) Permatasari, F. A.; Irham, M. A.; Bisri, S. Z.; Iskandar, F. Carbon-Based Quantum Dots for Supercapacitors: Recent Advances and Future Challenges. *Nanomaterials* **2021**, *11*, No. 91.
(30) Kuba, K.; Imai, Y.; Rao, S.; Gao, H.; Guo, F.; Guan, B.; Huan, Y.; Yang, P.; Zhang, Y.; Deng, W.; Bao, L.; Zhang, B.; Liu, G.; Wang, Z.; Chappell, M.; Liu, Y.; Zheng, D.; Leibbrandt, A.; Wada, T.; Slutsky, A. S.; Liu, D.; Qin, C.; Jiang, C.; Penninger, J. M. A Crucial Role of Angiotensin Converting Enzyme 2 (ACE2) in SARS Coronavirus-Induced Lung Injury. *Nat. Med.* **2005**, *11*, 875−879.
(31) Ogi, T.; Aishima, K.; Permatasari, F. A.; Iskandar, F.; Tanabe, E.; Okuyama, K. Kinetics of Nitrogen-Doped Carbon Dot Formation: Via Hydrothermal Synthesis. *New J. Chem.* **2016**, *40*, 5555−5561.
(32) Permatasari, F. A.; Nakul, F.; Mayangsari, T. R.; Aimon, A. H.; Nuryadin, B. W.; Bisri, S. Z.; Ogi, T.; Iskandar, F. Solid-State Nitrogen-Doped Carbon Nanoparticles with Tunable Emission Prepared by a Microwave-Assisted Method. *RSC Adv.* **2021**, *11*, 39917−39923.
(33) Permatasari, F. A.; Fukazawa, H.; Ogi, T.; Iskandar, F.; Okuyama, K. Design of Pyrrolic-N-Rich Carbon Dots with Absorption in the First near-Infrared Window for Photothermal Therapy. *ACS Appl. Nano Mater.* **2018**, *1*, 2368−2375.
(34) Santika, A. S.; Permatasari, F. A.; Umami, R.; Muyassiroh, D. A. M.; Irham, M. A.; Fitriani, P.; Iskandar, F. Revealing the Synergetic

https://doi.org/10.1021/acsomega.2c07398
ACS Omega 2023, 8, 10077−10085

Interaction between Amino and Carbonyl Functional Groups and Their Effect on the Electronic and Optical Properties of Carbon Dots. *Phys. Chem. Chem. Phys.* **2022**, *24*, 27163−27172.
(35) Umami, R.; Permatasari, F. A.; Muyassiroh, D. A. M.; Santika, A. S.; Sundari, C. D. D.; Ivansyah, A. L.; Ogi, T.; Iskandar, F. A Rational Design of Carbon Dots: Via the Combination of Nitrogen and Oxygen Functional Groups towards the First NIR Window Absorption. *J. Mater. Chem. C* **2022**, *10*, 1394−1402.
(36) Pan, X. w.; Xu, D.; Zhang, H.; Zhou, W.; Wang, L. h.; Cui, X. g. Identification of a Potential Mechanism of Acute Kidney Injury during the COVID-19 Outbreak: A Study Based on Single-Cell Transcriptome Analysis. *Intensive Care Med.* **2020**, *46*, 1114−1116.
(37) Lukassen, S.; Chua, R. L.; Trefzer, T.; Kahn, N. C.; Schneider, M. A.; Muley, T.; Winter, H.; Meister, M.; Veith, C.; Boots, A. W.; Hennig, B. P.; Kreuter, M.; Conrad, C.; Eils, R. SARS -CoV-2 Receptor ACE 2 and TMPRSS 2 Are Primarily Expressed in Bronchial Transient Secretory Cells. *EMBO J.* **2020**, *39*, No. e105114.
(38) Senthil Kumar, K. J.; Vani, M. G.; Wang, C. S.; Chen, C. C.; Chen, Y. C.; Lu, L. P.; Huang, C. H.; Lai, C. S.; Wang, S. Y. Geranium and Lemon Essential Oils and Their Active Compounds Down-regulate Angiotensin-Converting Enzyme 2 (ACE2), a SARS-CoV-2 Spike Receptor-Binding Domain, in Epithelial Cells. *Plants* **2020**, *9*, No. 770.
(39) Feng, T.; Ai, X.; An, G.; Yang, P.; Zhao, Y. Charge-Convertible Carbon Dots for Imaging-Guided Drug Delivery with Enhanced in Vivo Cancer Therapeutic Efficiency. *ACS Nano* **2016**, *10*, 4410−4420.
(40) Wang, L. F.; Sun, Y. Y.; Pan, Q.; Yin, Y. Q.; Tian, X. M.; Liu, Y.; Bu, T.; Zhang, Q.; Wang, Y. A.; Zhao, J.; Luo, Y. Diminazen Aceturate Protects Pulmonary Ischemia-Reperfusion Injury via Inhibition of ADAM17-Mediated Angiotensin-Converting Enzyme 2 Shedding. *Front. Pharmacol.* **2021**, *12*, 1−17.
(41) Tetlow, S.; Segiet-Swiecicka, A.; O'Sullivan, R.; O'Halloran, S.; Kalb, K.; Brathwaite-Shirley, C.; Alger, L.; Ankuli, A.; Baig, M. S.; Catmur, F.; Chan, T.; Dudley, D.; Fisher, J.; Iqbal, M. U.; Puczynska, J.; Wilkins, R.; Bygate, R.; Roberts, P. ACE Inhibitors, Angiotensin Receptor Blockers and Endothelial Injury in COVID-19. *J. Intern. Med.* **2021**, *289*, 688−699.
(42) Huang, M. L.; Li, X.; Meng, Y.; Xiao, B.; Ma, Q.; Ying, S. S.; Wu, P. S.; Zhang, Z. S. Upregulation of Angiotensin-Converting Enzyme (ACE) 2 in Hepatic Fibrosis by ACE Inhibitors. *Clin. Exp. Pharmacol. Physiol.* **2010**, *37*, e1−e6.
(43) Permatasari, F. A.; Umami, R.; Deliana, C.; Sundari, D.; Rona Mayangsari, T.; Ivansyah, A. L.; Muttaqien, F.; Ogi, T.; Iskandar, F. New Insight into Pyrrolic-N Site Effect towards the First NIR Window Absorption of Pyrrolic-N-Rich Carbon Dots *Nano Research* 2022 DOI: 10.1007/s12274-022-5131-7.
(44) Indriyati; Primadona, I.; Permatasari, F. A.; Irham, M. A.; Nasir, M.; Iskandar, F. Recent Advances and Rational Design Strategies of Carbon Dots towards Highly Efficient Solar Evaporation. *Nanoscale* **2021**, *13*, 7523−7532.
(45) Trott, O.; Olson, A. J. AutoDock Vina: Improving the Speed and Accuracy of Docking with a New Scoring Function, Efficient Optimization, and Multithreading. *J. Comput. Chem.* **2010**, *31*, 455−461.
(46) Peng, Z.; Han, X.; Li, S.; Al-youbi, A. O.; Bashammakh, A. S.; El-shahawi, M. S.; Leblanc, R. M. Carbon Dots: Biomacromolecule Interaction, Bioimaging and Nanomedicine. *Coord. Chem. Rev.* **2017**, *343*, 256−277.
(47) Bosso, M.; Thanaraj, T. A.; Abu-Farha, M.; Alanbaei, M.; Abubaker, J.; Al-Mulla, F. The Two Faces of ACE2: The Role of ACE2 Receptor and Its Polymorphisms in Hypertension and COVID-19. *Mol. Ther.–Methods Clin. Dev.* **2020**, *18*, 321−327.
(48) Kulemina, L. V.; Ostrov, D. A. Prediction of Off-Target Effects on Angiotensin-Converting Enzyme 2. *SLAS Discovery* **2011**, *16*, 878−885.

https://doi.org/10.1021/acsomega.2c07398
ACS Omega 2023, 8, 10077−10085